35th Annual International Conference of the IEEE EMBS
Osaka, Japan, 3 - 7 July, 2013

Influences of Blood Flow Changes in Cerebrospinal Fluid and Skin Layers on Optical Mapping*

Shuping. Wang, Yoko. Hoshi, and Yukio. Yamada

Abstract— **In optical mapping for imaging brain activity, the effect of blood flow changes in superficial tissues such as the cerebrospinal fluid (CSF) and skin layers should be considered. However, it is difficult to know those changes in *in vivo* experiments. To investigate the influence of blood flow changes in CSF and skin layers on optical mapping, we perform numerical simulations of optical mapping by solving the photon diffusion equation for layered-models simulating human heads using the finite element method (FEM). The results show that mapping images of activated region in the gray matter layer are affected by the existence of blood vessels in CSF layer and by the blood flow changes in the skin layer. The increases in both the vessel size and vessel absorption coefficient reduce the sensitivity of the mapping images to the brain activity in the gray matter. On the other hand, the increase in the vessel volume fraction in the skin layer increases the sensitivity of the mapping images.**

I. Introduction

Functional brain imaging is realized with near-infrared spectroscopy by measuring hemodynamic responses to neuronal activation in the cerebral cortex. Optical mapping can image brain activation two-dimensionally along the head surface by detecting the intensity changes of light that passes through the brain [1-2]. Changes in the intensities of the light detected by pairs of source and detector optical fibers can be used to estimate regional brain activation. Due to its cost efficiency, its less restriction on the subjects and more compact system setup than other modalities, optical mapping has a high potential as a neuroimaging technology.

A major disadvantage of optical mapping comes from the need of irradiating near-infrared light through the superficial tissues, such as the skin, skull and CSF layers over the brain. Previous studies have shown that the variations in thicknesses of the skin, skull and CSF layers affect the optical mapping images [3-4]. In addition, optical mapping is sensitive to blood vessels in the superficial tissues because oxygenated and deoxygenated hemoglobins are the dominant chromophores in the near infrared window. The existence of the blood vessels and the hemodynamic changes in the superficial layers should be taken into account, in particular, the existence of the pial vessel in the CSF layer, and the change in the blood volume fraction induced by the vasodilation and vasocontraction in the skin layer.

*Research supported by JSPS KAKENHI No. 22360087.

Shuping.Wang and Yukio. Yamada is with the Department of Mechanical Engineering and Intelligent Systems, University of Electro-Communications, Tokyo, Japan. (corresponding author to provide phone: +81-42-443-5338; e-mail: wang@mce.uec.ac.jp), (Yukio. Yamada, e-mail: wang@mce.uec.ac.jp) .

Yoko. Hoshi is with the Integrated Neuroscience Research Project Tokyo Metropolitan Institute of Medical Science, Tokyo, Japan (e-mail: hoshi-yk@igakuken.or.jp).

Several methods have been proposed to eliminate the effect of the blood flow changes in the skin layer, including multiple source-detector distance and independent component analysis (ICA) [5-6]. The sensitivity of the NIRS signal to the hemodynamic changes in the skin layer was found to be dependent on the source-detector distance and the model used for estimation [7-9]. Optical mapping, in which the source-detector distance of 30mm is known to be the optimum distance for near-infrared light to penetrate into the brain, cannot tell what layer the changes in the detected light come from. Numerical simulation of optical mapping is an effective way to assess the sensitivity of detected signal to the brain activation, because the signals specifically arising from the brain tissue cannot be detected experimentally. In contrast, the origins of the signals can be estimated by numerical simulation.

Previous reports of numerical simulations of optical mapping assumed that only the light absorption in the brain changed due to brain activation and that the optical properties of the superficial layers unchanged [3.4]. The purpose of this study is to investigate the influence of blood flow changes in the cerebrospinal fluid (CSF) and skin layers on mapping images by numerical simulations. Three-dimensional (3D) head models are constructed to calculate light propagation in the head. The influences on the mapping images are discussed and used to evaluate the mapping images quantitatively.

II. Method of Numerical Simulation

A. Theory of optical mapping

In optical mapping, the change in the intensity of the detected light is measured to obtain the absorption change in the brain. Source light (λ) irradiates a head surface and is detected at the distance of about 30mm from the source position. The optical density at the wavelength of λ, $OD(\lambda)$, is defined by (1),[10]

$$OD(\lambda) = -\ln \frac{\Phi(\lambda)}{\Phi_0(\lambda)} \tag{1}$$

where $\Phi_0(\lambda)$ and $\Phi(\lambda)$ are the source and detected light intensities, respectively. Optical mapping uses the measured data of the differences in the OD between the activation and rest states of brain, $\Delta OD(\lambda)$, which is given by (2),

$$\Delta OD(\lambda) = OD_a(\lambda) - OD_n(\lambda) = -\ln \frac{\Phi_a(\lambda)}{\Phi_n(\lambda)} \tag{2}$$

Where λ is the wavelength of light, Φ is the measured light intensity, and the subscripts "a" and "n" indicate the activation and rest states, respectively. By use of the modified Beer-Lambert law, $\Delta OD(\lambda)$ is related to the concentration changes in the oxy- and deoxy-hemoglobin as in (3),

$$\Delta OD(\lambda) = \varepsilon_{HbO_2}(\lambda)(C^a_{HbO_2} - C^n_{HbO_2})l + \varepsilon_{Hb}(\lambda)(C^a_{Hb} - C^n_{Hb})l \quad (3)$$
$$= \varepsilon_{HbO_2}(\lambda)\cdot\Delta C_{HbO_2}\cdot l + \varepsilon_{Hb}(\lambda)\cdot\Delta C_{Hb}\cdot l$$

Where $\varepsilon(\lambda)$ is the molar extinction coefficient [mm-1mM-1], C is the molar concentration [mM], l is the effective pathlength [mm], and the subscripts "Hb" and "HbO_2" denote oxy- and deoxy-hemoglobin, respectively.

In optical mapping, measurements of ΔOD(λ) are made at two wavelengths of $\lambda = \lambda_1$ and λ_2, and the values of $\Delta C_{HbO2}\cdot l$ and $\Delta C_{Hb}\cdot l$ are obtained by solving the two simultaneous equations of (3) for λ_1 and λ_2. These values of $\Delta C_{HbO2}\cdot l$, $\Delta C_{Hb}\cdot l$ or $\Delta C_{Hbt}\cdot l$ ($=\Delta C_{HbO2}\cdot l + \Delta C_{Hb}\cdot l$) are allocated at the midpoints between the neighboring source and detector positions which are called the data points. Then these values at the data points are used to construct 2-D mapping images by interpolation. In this study, light with a single wavelength of λ_3 = 805 nm which is the isobestic point of the absorption spectra of *Hb* and *HbO2* (i.e., $\varepsilon_{HbO2}(\lambda_3) = \varepsilon_{Hb}(\lambda_3)$) is used, and only the mapping images of $\Delta C_{Hbt}\cdot l \cdot \varepsilon_{Hb}(\lambda_3) = \Delta OD(\lambda_3)$ are given for simplicity.

B. *Modeling of optical mapping*

The arrangement of the source and detector probes in the simulation is shown in Fig. 1. Sixteen probes with eight sources and eight detectors are used. The separation of each source-detector pair is fixed at 30mm. The whole area where the probes cover is the square of 90 mm by 90 mm. A total of 24 data points are allocated as the midpoints between the neighboring source and detector for the arrangement of 8 source-detector pairs. The area of simulation of light propagation is 150 mm by 150 mm as the result of 30mm extension at all sides of the area that the probes cover.

Figure 1. Arrangement of the sources and detectors, data points, and active regions.

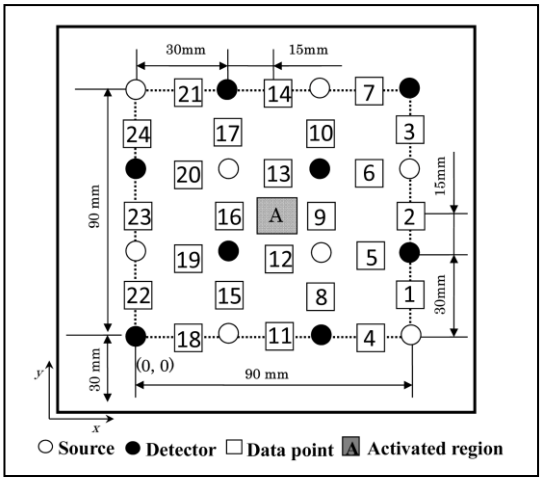

Light propagation in tissues is assumed to be governed by the steady state photon diffusion equation, (4)

$$\nabla[D(r)\nabla\phi(r)] - \mu_a(r)\phi(r) = 0 \quad (4)$$

where r is the position vector, ϕ is the fluence rate, $D(r) = 1/(3\mu_s')$ is the diffusion coefficient, μ_s' and μ_a are the reduced scattering and absorption coefficients, respectively. A commercially available software (COMSOL Multiphysics) was used to solve (4) by FEM. The number of FEM elements was 10^5.

C. *Models of human head with activated region, blood vessel in the CSF and blood flow changes in the skin*

The simulation model of the human head for optical mapping is shown in Fig. 2. The head model consists of five layers, skin, skull, CSF, gray matter and white matter layers. When the brain is activated, we assume the existence of activated regions in the gray matter with a higher absorption coefficient than that of the surrounding brain tissues and with the size of 10 mm×10 mm×3.5 mm [11].

To illustrate how the existence of a blood vessel in the CSF layer affect the optical images of active region in the gray matter, we used four head models of (C1) with no blood vessel in the CSF layer, (C2) with a 1mm-side square blood vessel having μ_a of 0.13 mm^{-1} in the CSF layer, (C3) with a 1mm-side square blood vessel having μ_a of 0.27 mm^{-1} in the CSF layer, (C4) with a 1mm×2mm rectangular blood vessel having μ_a of 0.13 mm^{-1} in the CSF layer, and (C5) with a 1mm×2mm rectangular blood vessel having μ_a of 0.27mm^{-1} in the CSF layer. The blood vessels are all located above the center of the active region.

Figure 2. Simulation models of human heads having five layers; skin, skull, CSF, gray matter, and white matter layers.

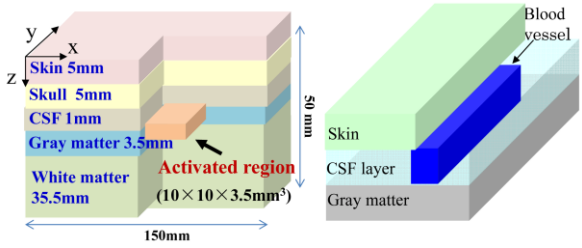

To study how the blood flow changes in the skin layer influence the mapping images, we assume that the blood vessels are homogeneously distributed in the skin layer with a small volume fraction and that the change in the blood flow is represented by the changing the blood volume fraction (f_B) and blood oxygenation which result in the change in the absorption coefficient of the skin layer. Three cases are assumed; i.e., case (S1) where μ_a of the skin layers is 0.030 mm^{-1} without including the blood vessel, case (S2) where μ_a is 0.037 mm^{-1}for a standard f_B of 10% and blood oxygen saturation (S_{O2}) of 70%, and case (S3) where μ_a is 0.046 mm^{-1} for an increase in f_B to 18% with S_{O2} of 81 % in the skin layer [12-14]. The standard optical properties of each layer at the wavelength of 805nm are listed in Table 1.

TABLE I. OPTICAL PROPERTIES OF THE HEAD LAYERS

Layer	μ_a(mm^{-1})	μ_s' (mm^{-1})
Skin	0.03	0.73
Skull	0.012	1.8
CSF layer	0.002	0.3
Gray matter	0.036	2.3
White matter	0.014	9.1
Activated region	0.052	2.3

III. Results and Discussions

A. Influence of the blood vessel in CSF layer on mapping images

Fig. 3(A) shows the simulation results of the mapping images (A) case (C1) without the blood vessel, (B) case (C2), (C) case (C3), (D) case (C4) and (E) case (C5) with blood vessels. Compared to case (C1) without the vessel, the existence of the vessel, cases (C2), (C3), (C4) and (C5), reduced the sensitivity of the mapping images to the brain activity. When μ_a increased from 0.13 mm^{-1} for case (C2) to 0.27 mm^{-1} for case (C3) with the same 1mm-side square vessel, the sensitivity of the mapping images reduced as μ_a increased. Keeping μ_a constant as 0.27 mm^{-1}, the sensitivity of the images of case (C5) with the 1mm×2mm rectangular blood vessel decreased from case (C3) with the 1-mm-side square blood vessel. In addition, with the approximately equal blood volume for the case (C3) and (C4), the mapping images are almost the same. This results show that the effect of blood vessel in CSF layer on mapping images is dependent on the whole blood volume.

To show the effect clearly, Fig. 3(F) displays the lateral profile of ΔOD along the horizontal lines through the centers of the active region as indicated in Fig. 3(A).ΔOD for case (C1) is the largest among all the cases. Increasing both the absorption coefficient and size of the vessel decreases the value of ΔOD.

Figure 3. Influences of the existence of a blood vessel in the CSF layer, (A) case (C1) without a blood vessel, (B) case (C2) with a 1mm-side square blood vessel with μ_a = 0.13 mm^{-1}, (C) case (C3) with a 1mm-side square blood vessel with μ_a = 0.27 mm^{-1}, (D) case (C4) with a 1mm×2mm rectangular blood vessel with μ_a = 0.27 mm^{-1}, (E) the profiles of ΔOD along the horizontal lines through the center of the active region, as indicated in (A).

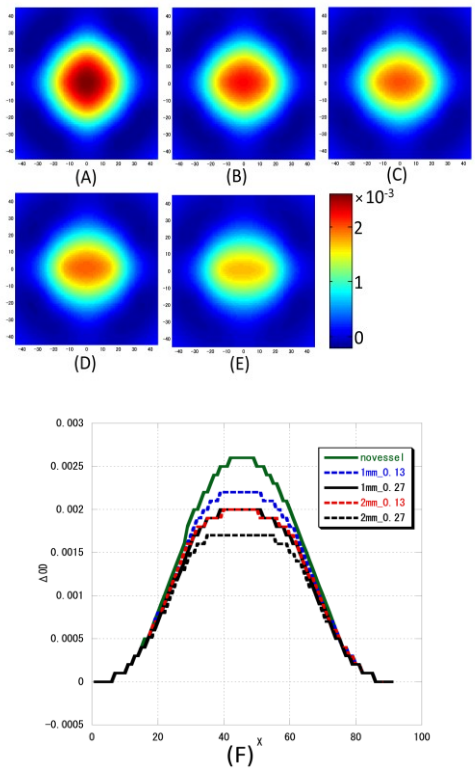

It can be said that the existence of a blood vessel in the low-scattering and low-absorbing CSF layer affects light passing through the gray matter. If μ_a of the vessel increases by some reasons, the probability of light passing through the gray matter decreases, therefore resulting in the decrease in the sensitivity of the mapping images to the brain activation.

B. Influence of blood flow changes in skin layer in mapping images

Fig. 4(A), (B) and (C) shows the simulation results of the mapping images for cases (S1), (S2) and (S3) where μ_a of the skin layer changes. Comparing with case (S1) without the vessel in the skin layer, ΔOD increased for cases (S2) and (S3) where the blood volume fraction, f_B, increased. With the activation of blood vessel, μ_a of the skin layer increases from case (S2) to case (S3), and the sensitivity of the mapping images increases.

Fig. 4(D) shows the lateral profiles of ΔOD along the horizontal lines through the center of the active region. The peak values of ΔOD increased with the increase in f_B in the skin.

Figure 4. Influences of the change in μ_a of the skin layer. (A) case (S1) with μ_a = 0.030 mm^{-1}, (B) case (S2) with μ_a = 0.056 mm^{-1}, (C) case (S1) with μ_a = 0.086 mm^{-1}, and (D) the lateral profiles of ΔOD for cases (S1) (green), (S2) (red) and (S3) (black).

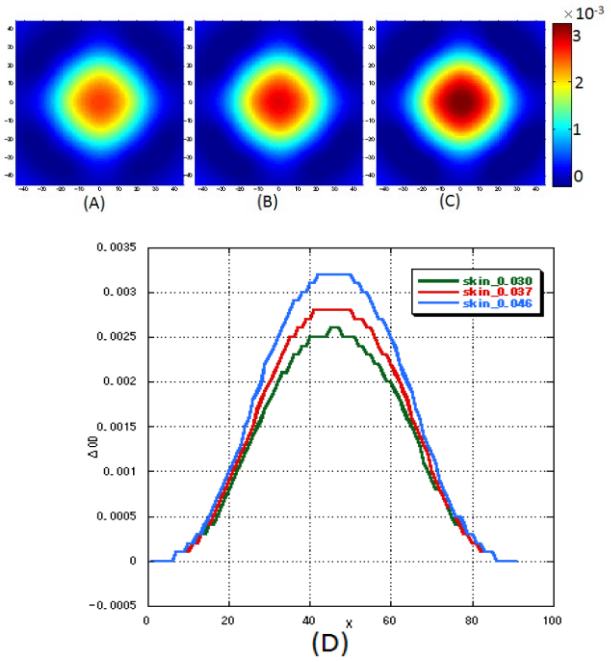

The simulation results show that the mapping images have a strong dependency on the change in the blood volume fraction in the skin layer. The increase in μ_a of the skin layer increases the sensitivity of the mapping images to the brain activity in the gray matter. Intuitively, these results look unreasonable because light penetration to the deeper tissues is blocked more by higher absorption by the skin layer. In order to understand these results, OD_a and OD_n measured at the 24 data points are plotted in Fig. 5(A), and $\Delta OD = OD_a - OD_n$ in Fig. 5(B) for the three cases (S1), (S2) and (S3). The abscissa corresponds to the number of the data points shown in Fig. 1. As seen from Fig. 5(A), the differences between OD_a and

OD_n with the same μ_a of the skin layer are very small compared to their magnitudes, and OD_a and OD_n look almost the same although their magnitudes greatly decrease with the increase in μ_a of the skin layer. However, Fig. 5(B) shows that ΔOD increases with the increase in μ_a of the skin layer resulting in the higher sensitivity of the mapping images to the brain activity.

These results may be phenomenologically understood as follows. By increasing μ_a of the skin layer, the contribution of the skin layer to the attenuation of the measured light intensities relatively decreases compared to those of the deeper layers. Then the change in the absorption in the gray matter leads to larger ΔOD than that with lower absorption in the skin layer. This qualitative estimation can be confirmed quantitatively by calculating the photon pass probability between the source and detector positions for future study.

Figure 5. (A) Φ_n and Φ_a and (B) ΔOD at the 24 data points for cases (S1), (S2) and (S3).

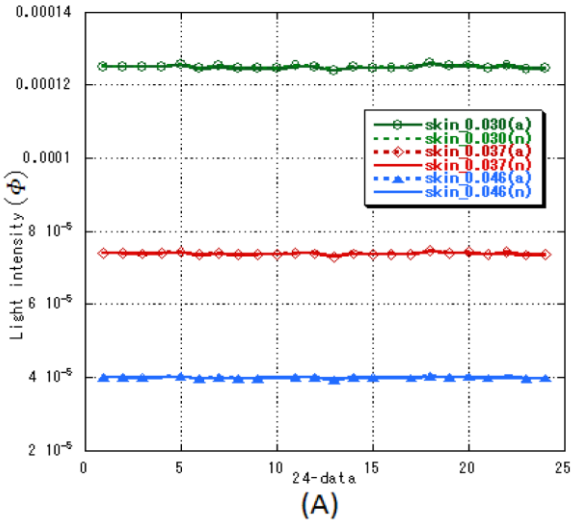

IV. Conclusion

Both the pial vessels in the CSF layer and blood flow changes in the skin layer affect the images of optical mapping. In particular, it has been found that the increase in the blood volume fraction in the skin layer increases the sensitivity of the mapping images to the brain activity while the existence of the blood vessel in the CSF layer decreases the sensitivity of the mapping images to the brain activity. To extract the true activity of brain from optical mapping images, these influences from the superficial layers should be eliminated. Future studies are needed to remove the influences and improve the performances of the mapping images.

References

[1] A. Maki, Y. Yamashida, Y. Ito, E. Watanabe and H. Koizumi, "Spatial and temporal analysis of human motor activity using noninvasive NIR topography," Med.phys., vol. 22, Dec. 1995, pp. 1997-2005.

[2] M. Ferrari and V. Quaresima, "A brief feview on the history of human functional near-infrared spectroscopy (fNIRS) development and fields of application," NeuroImage, vol. 63, Nov. 2012, pp. 921-935.

[3] E. Okata and D. T. Delpy, "Near-infrared light propagation in an adult head model. II. Effect of superficial tissue thickness on the sensitivity of the near-infrared spectroscopy signal," Appl. Opt, vol. 42, Jun. 2003, pp.2915-2922.

[4] S. Wang, N. Shibahara, D. Kuramashi, S. Okawa, N. Kakuta, E, Okata, A. Maki and Y. Yamada, "Effects of Spatial variation of skull and cerebrospinal fluid layer in optical mapping of brain activities," Opt. Rev, vol. 17, Jul. 2010, pp. 410-420.

[5] Q. Zhang, G. E. Strangman and G. Ganis, "Adaptive filtering to reduce global inference in non-invasive NIRS measures of brain activation: How well and when does it work?" NeuroImage, vol. 45, Jan. 2009, pp. 788-794.

[6] N. M. Gregg, B. R. White, B. W. Zeff, A. J. Berger and J. P. culver, "Brain specificity of diffuse optical imaging: improvements from superficial signal regression and tomography," Front. Neurosci. vol. 2, Jul. 2010, pp. 1-8.

[7] E. Kirilina, A. Jelzow, A. Heine, M. Niessing, H. Wabnitz, R. Bruhl, B. Ittermann, A. M. Jacobs and I. Tachtsidis, "The physiological origin of task-evoked systemic artefacts infunctional near infrared spectroscopy," NeuroImage, vol. 61, Mar. 2012, pp. 70-81.

[8] T. Takahashi, Y. takikawa, R. Kawagoe, S. Shibuya, T. Iwano and S. Kitazawa, "Influence of skin blood flow on near-infrared spectroscopy signals measured on the forehead during a verbal fluency task," NeuroImage, vol. 57, May. 2011, pp. 991-1002.

[9] M. Dehaes, L. Gagnon, F. Lesage, M. P. Issac, A. Vignaud, R. Valabregue, R. Grebe, F. Wallois and H. Benali, "Quantitative investigation of the effect of the extra-cerebral vasculature in diffuse optical imaging: a simulation study," Bio. Opt. Exp, vol. 2, Mar. 2011, pp. 680-695.

[10] D. T. Delpy, M. Cope, P. van der Zee, S. R. Arridge, S. Wray and J. S. Watt, "Estimation of optical pathlength through tissue from direct time of flight measurement ," Phys. Med. Bol, vol.33, Jul. 1988, pp. 1443-1442.

[11] T. Yamamoto, A. Maki, T. Kadoya, Y. Tanikawa, Y. Yamasa, E. Okada and H. Koizumi, "Arranging optical fibers for the spatial resolution improvement of topographical images," Phys. Med. Bol, vol.47, Sep. 2002, pp. 3429-3440.

[12] S. L. Jacques, "Optical assessment of cutaneous blood volume depends on the vessel size distribution: a computer simulation study," J. Biophotonics, vol. 3, Dec. 2010, pp. 75-81.

[13] H. Liu, B. Chance, A. H. Hielscher, S. L. Jacques and F. K. Tittel, " Influence of blood vessels on the measurement of hemoglobin oxygenation as determined by time-resolved reflectance spectroscopy," Am. Assoc. Phys. Med, vol. 22, Aug. 1995, pp. 1209-1217.

[14] S. N. Davie and H. P. Grocott, "Impact of extracranial contamination on regional cerebral oxygen saturation: A comparison of three cerebral oximetry technologies," Anesthesiology, vol. 116, Apr. 2012, pp. 1-7.